PADEU | PADEU **15**, 35 (2005)
ISBN 963 463 557

Impulsively heated solar coronal plasma

C. A. Mendoza-Briceño

Solar Physics & upper-Atmosphere Research Group, Department of Applied Mathematics, University of Sheffield, Hicks Building, Hounsfield Road, Sheffield, S3 7RH, England, UK

E-mail: c.mendoza@sheffield.ac.uk

Abstract
The dynamics response of the solar coronal plasma in a magnetic flux tube undergoing impulsive heating through the release of localized Gaussian energy pulses near the loop's footpoints is investigated. It was found that when a discrete number of randomly spaced pulses is released, loops heat up and stay at coronal temperatures for the whole duration of the impulsive heating stage provided that the elapsing time between pulses is less than a critical one. For elapsing times longer than this critical value, coronal temperatures can no longer be maintained and the loop apex cools down reaching chromospheric temperatures. For a large number of pulses having a fully random spatio-temporal distribution, the variation of the temperature along the loop is highly sensitive to the spatial distribution of the heating. As long as the heating concentrates more and more at the loop's footpoints, the temperature variation is seen to make a transition from that of a uniformly heated loop to a flat, isothermal profile along the loop length. Concentration of the heating at the footpoints also results in a more frequent appearance of rapid and significant depressions of the apex temperature during the loop evolution, most of them ranging from $\sim 1.5 \times 10^6$ to $\sim 10^4$ K and lasting from about 3 to 10 minutes. This behavior strongly resembles the intermittent variability of coronal loops inferred from SoHO observations in active regions of the solar atmosphere.
Keywords: *Sun: atmosphere, transition region, hydrodynamics, Sun: corona*

1 Introduction

The heating of the solar coronal plasma remains one of the most challenging problem in solar physics. Several heating mechanism have been proposed but recent interest has centered on the idea that flarelike discrete events heat the solar corona (Parker 1988). High resolution observations by space imaging telescope and spectrometers have revealed a variety of very small scale activities at transition region that may serve as building blocks of the heating mechanism (Innes et al. 1997; Harrison 1997; Pérez et al. 1999; Erdélyi et al. 2001). Numerical models aimed at studying the nature of localised energy deposition and their contribution to the coronal heating mechanisms have been proposed e.g. by Sarro et al. (1999), Teriaca et al. (1999), Roussev et al. (2001a,b), Bradshaw & Mason (2003), whereas Walsh & Galsgaard (2000) studied the response of the coronal plasma to dynamical heat input generated by the flux-braiding model. More recently, Mendoza-Briceño, Erdélyi, & Sigalotti (2002) and Mendoza-Briceño, Sigalotti, & Erdélyi (2003) investigated the hydrodynamical behavior of closed magnetic loops undergoing impulsive heating near the footpoints. They found that when a discrete number ($\lesssim 10$) of pulses are injected either periodically or randomly in space with constant elapsing times, the average plasma temperature stays over a million kelvins for the duration of the impulsive heating, with approximate *isothermal profiles* along the upper, hot loop segments. These temperature profiles are consistent with a heating function that decays *exponentially* from the loop's footpoints towards the apex in good agreement with observations of *TRACE* loops (Aschwanden et al. 2001).

In this paper, we report on the response of the coronal loop plasma to spatio-temporal microscale heating near the footpoints. First, we explore the effects of increasing the constant elapsing time between successive energy inputs on catastrophic cooling for a discrete number of randomly spaced pulses and varied total length of the loop. Second, we consider models with a large number of pulses where the energy releases are now applied randomly in space and time as well as in their occurrence at one or both footpoints. This gives rise to loop evolutions in which the heat injections are fully random and asymmetric. Finally, for these latter models we also consider the effects of varying the length of the bottom loop segments along which the localized pulses are randomly distributed. This allows for hypothetical loop models undergoing impulsive heating at the footpoints and across the transition region.

2 Hydrodynamic loop model

Coronal loops are modelled as semicircular magnetic flux tubes of constant cross section anchored in the photosphere. Plasma motion along the tube can be approximately described by solving numerically the standard set of transport equations for mass, momentum, and energy in one space dimension, including the effects of heat conduction, radiative cooling, and heating.

In this paper we assume that the heating deposition has a spatial and temporal dependence given by

$$H(s,t) = h_0 + H_0 \sum_{i=1}^{n} \exp[-\alpha(t-\tau_i)] \times$$

$$\times \left\{ \lambda_{l,i} \exp\left[-\frac{(s-s_{l,i})^2}{\beta^2} \right] + \lambda_{r,i} \exp\left[-\frac{(s-s_{r,i})^2}{\beta^2} \right] \right\} , \qquad (1)$$

where t is time, s the curvilinear coordinate along the field line, $h_0 = 3.6 \times 10^{-4}$ ergs cm^{-3} s^{-1} is the uniform background heating rate, $H_0 = 30$ ergs cm^{-3} s^{-1} determines the maximum amplitude of the impulsive heating, $\beta \approx 3.6 \times 10^6$ cm is the spatial width of the heating, and $\alpha = -\ln(0.1)/\Delta t$ so that 90% of the total energy is deposited during a finite time taken to be $\Delta t = 150$ s. We use heat pulses of total energy $E_{tot} \sim 10^{25}$ ergs. The elapsing time τ_i between successive pulses is chosen randomly within the interval $20 \leq \tau_i \leq 190$ s. In addition, the pulses are centered at distances $s_{l,i} = \Delta L \cdot \mathrm{RAN}_{l,i}$ and $s_{r,i} = L(1 - \Delta L \cdot \mathrm{RAN}_{r,i})$ from the left and right footpoints, respectively, where RAN_l and RAN_r define different sequences of random numbers between 0 and 1 allowing for asymmetrical heat injections near the footpoints. Finally, the parameters $\lambda_{l,i}$ and $\lambda_{r,i}$ are randomly chosen to be either 0 or 1 so that the injections may arbitrarily happen at one or both footpoints. For each model calculation four distinct sequences of $n = 5000$ random numbers were employed to determine the parameters τ_i, $s_{l,i}$, $s_{r,i}$, and ($\lambda_{l,i}$, $\lambda_{r,i}$) in Eq. (1). In all models with constant τ_i, the first pulse is always released at the beginning ($t = 0$) of the calculation.

To solve the hydrodynamic loop equations, we use the 1D finite-difference code employed in previous models of impulsively heated loops (Mendoza-Briceño et al. 2002, 2003) and adopt many of the same parameters and assumptions that were made in those earlier simulations with this code. We refer the reader to Sigalotti & Mendoza-Briceño (2003) for a detailed account of the numerical methods and tests. All of our model calculations begin with an initial loop configuration in hydrostatic equilibrium. The initial cool atmosphere (≈ 0.55 MK) is such that the base pressure is always at 0.1 dyne cm^{-2} and is consistent with the value chosen for the background volumetric heating rate h_0. As in previous models, the total length of our basic loop model is $L = 1.0 \times 10^9$ cm (10 Mm), excluding the chromosphere. Additional calculations are presented for loops with total length $L = 5$, 20, and 30 Mm. Appropriate boundary conditions are applied at both footpoints by fixing the density and temperature there to their initial equilibrium values. Given that $p \propto \rho T$, this results in a constant pressure at $s = 0$ and L. In this way, the presence of a deep chromosphere is mimicked by evolving the velocity at the loop ends, thereby allowing for a flow of mass across the footpoints. All models are initialized the same way and the background heating is always maintained in which case we expect the loop model to return to the equilibrium density and temperature associated with this heating rate. Models with a discrete number (= 10) of randomly spaced pulses are all identical except for the constant

elapsing time τ_i between consecutive heat injections, which is varied from 60 to 240 s for the $L = 5$ and 10 Mm loops and to higher values (up to 300 s) for the $L = 20$ and 30 Mm cases. Finally, the model calculations with a large number (up to 1000 or more) of impulsive injections distributed randomly in space, time, and in their occurrence close to the footpoints all start with $L = 10$ Mm; the only variations in the simulations being the seeds generating the four distinct sequences of random numbers employed in Eq. (1) and the length $\Delta L/L$(=0.1, 0.2, 0.3, or 0.5) of the bottom loop segments along which the pulses are injected.

3 Results and Discussion

Mendoza-Briceño et al. (2003) investigated the evolution of a 10 Mm loop when 10 randomly spaced pulses were released near the footpoints over loop segments of length $0.1L$ and with constant elapsing times between successive injections of either 60 or 120 s. It was found that the instantaneous temperature profiles of the evolving loops were characterized by the appearance of localized thermal bumps along their hot coronal segments. Such bumps bear a strong resemblance with the intermittent behavior detected by Patsourakos & Vial (2002) from their analysis of light curves obtained in the O IV and Ne VIII transition region and low corona emission lines, as recorded by *SOHO*/SUMER in a quiet Sun region. The observed bursts exhibit a rather random temporal variation and are presumably due to intermittent energy release followed by its dissipation. In this way, Patsourakos & Vial (2002) concluded that the intermittency of the examined signals is related to well-known types of transition events in the corona such as explosive events, blinkers, and micro/nanoflares.

In this paper we further investigate the existence of a critical value of τ_i by performing further simulations of the 10 Mm loop model along a sequence of increasing constant elapsing times up to $\tau_i = 240$ s. In particular, Fig. 1a shows the evolution of the loop temperature when the time interval between the heat pulses is of 180 s. In this case, the impulsive heating can maintain the overall loop temperature at around 1.5 MK for about 1700 s. As expected the loop temperature achieved is lower compared to models having shorter elapsing times. After 1700 s, the loop cools down and returns to the initial equilibrium atmosphere, which is maintained until the termination of the calculation at 4000 s. The contour plot in Fig. 1a depicts the temperature variation during the impulsive heating phase. It is interesting to note the oscillatory behavior of the 0.5 MK contour line after about 2000 s, when the perturbations are relaxed and the loop returns to its equilibrium state. Similar qualitative trends are found for longer elapsing times up to the critical value of $\tau_i \approx 215$ s. For values higher than this, the loop is maintained at coronal temperatures only for the duration of the first two pulses. Soon after, the top temperature suddenly drops below the initial state towards typical chromospheric values.

When the elapsing time is further increased to $\tau_i = 240$ s, the evolution produced

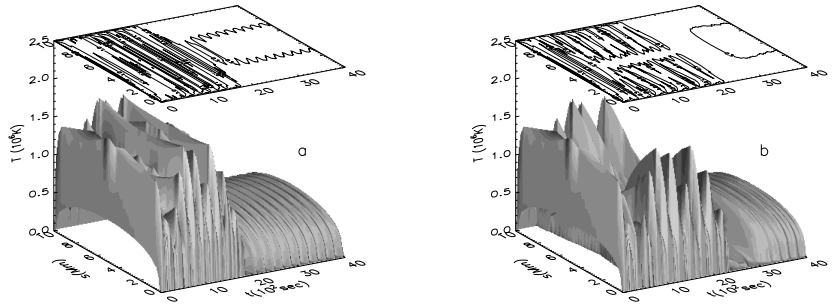

Figure 1: *Evolution of the temperature when* 10 *pairs of heat pulses are injected randomly over a segment of length* $0.1L$ *from each footpoint in a loop model of total length* $L = 10$ *Mm. The time interval between successive injections are of* 180 *s (a) and* 240 *s (b), with the first pair of pulses being released at the beginning of the evolution* ($t = 0$)*. A projected contour plot is shown for the temperature variations, where only contour lines for* 0.5*,* 1.0*, and* 1.5 *MK are shown.*

is qualitatively similar (see Fig. 1b). In this case, however, the cooling of the top loop segments lasts for a longer period ($\sim$ 1900 s) until the last pair of pulses is released (see Fig 2a). The spatial extent of the cool region around the loop apex is clearly evidenced by the temperature contour plot. We estimate that about 20% of the loop undergoes runaway cooling.

The critical elapsing time beyond which runaway cooling occurs is seen to depend on the total loop length. In particular, we find that loop models with the same heating parameters and increasing length experience catastrophic cooling at progressively higher critical elapsing times. For loops of length $L = 5$ Mm, the critical elapsing time is $\tau_i \approx 175$ s. This value rises to about 215, 240, and 263 s for loops of length 10, 20, and 30 Mm, respectively. Loops with the same subcritical value of τ_i and varied length evolve in a qualitatively similar fashion as we may see by comparing the time variations of the apex temperature depicted in Figs. 2*a* and *b* for $\tau_i = 120$ and 180 s. Since the timescale for heat conduction is $\tau_{cond} \propto \rho L^2$, conductive cooling is much more effective in the shorter than in the longer loops. This explains why during the heating stage the apex temperature in the 20 Mm loop oscillates about higher coronal values compared to the 10 Mm model. Similar trends are also seen when comparing the other model evolutions for $L = 5$ and 30 Mm. Larger values of the critical elapsing time are therefore required in the longer loops to allow conductive cooling have enough time to bring the loop apex past the equilibrium point, where radiative losses dominate and eventually induce the runaway cooling of the loop summit.

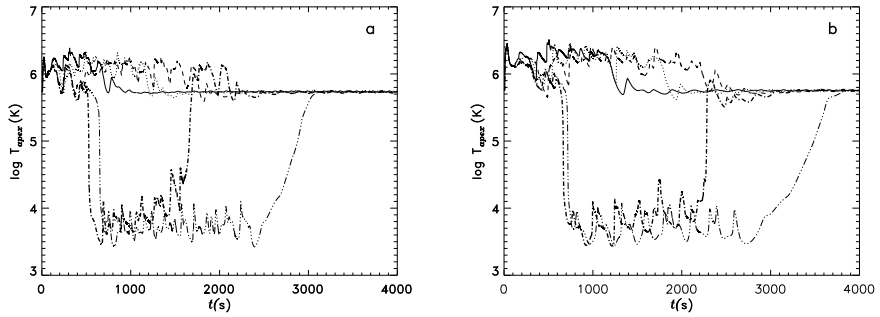

Figure 2: *Time variation of the apex temperature for loop models of total length (a)* $L = 10$ *Mm and (b)* $L = 20$ *Mm, undergoing impulsive heating through the release of* 10 *randomly spaced pulses near both footpoints. The elapsing time* τ_i *between successive pulses is of* 60 *s (solid line),* 120 *s (dotted line),* 180 *s (dashed line),* 220 *s (dot-dashed line), and* 240 *s (triple-dot-dashed line) in (a) and* 120 *s (solid line),* 180 *s (dotted line),* 240 *s (dashed line),* 245 *s (dot-dashed line), and* 260 *s (triple-dot-dashed line) in (b). Catastrophic cooling to temperatures* $\sim 10^4$ *K is evident for* $\tau_i = 220$ *and* 240 *s in (a) and* $\tau_i = 245$ *and* 260 *s in (b).*

We now consider the evolution of the 10 Mm loop model when it is heated by a large number of pulses distributed randomly in space and time near the footpoints. In contrast with the previous models, the pulses may not be simultaneous in the sense that they could appear randomly at one or both footpoints. The randomness in time is obtained by choosing arbitrarily the elapsing time between consecutive injections from the interval $20 \leq \tau_i \leq 190$ s. These values are all below the critical one for which we would expect the loop to undergo catastrophic cooling to chromospheric temperatures. Figure 3 shows the resulting temperature evolution for this loop model up to 15000 s, when more than about 1000 pulses have been released. We may see that the hottest segments of the loop reach temperatures higher than 1.5 MK, which are maintained until the termination of the calculation. When the randomness of the impulsive heating is varied, the evolution undergoes only quantitatively small changes. For instance, an obvious change involves differences in the spatio-temporal distribution of the thermal bumps which certainly modify the instantaneous shape of the temperature profiles when compared at identical evolutionary times. The variation of the apex density and temperature with time for the three model calculations is shown in Fig. 4. One important feature in these plots is the sporadic appearance of temperature drops accompanied by corresponding density rises. That is, during its impulsive heating the loop apex suddenly cools to temperatures $\gtrsim 10^4$ K and reheats to coronal temperatures

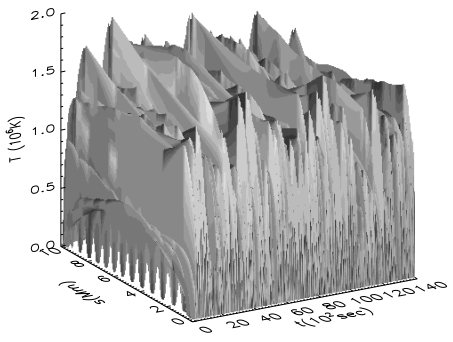

Figure 3: *Evolution of the loop temperature when a large number of heat pulses with a random distribution in space, time, and in their occurrence at one or both footpoints, is injected over a segment of length* $0.1L$ *from the feet in a loop model of total length* $L = 10$ *Mm.*

in a very short timescale. These variations in the local thermodynamic properties may be related to the observed rapid time variability of coronal loops detected in active regions of the solar atmosphere, which involves temperature variations in the interval from $\sim 10^4$ to $\sim 2.7\times10^6$ K (Kjeldseth-Moe & Brekke 1998). The predicted timescales for these rapid variations are of $\sim$ 3–10 min, which are towards the lower end of the range inferred observationally ($\sim$ 10–30 min). This implies that a loop at a given temperature that is missing in one location at a particular time may be present at another time. Also note that the number of the temperature depressions is related to the spatio-temporal dependence of the impulsive heating. We next consider the effects of varying the length ΔL of the bottom loop segments along which the pulses are randomly distributed for the same evolution model of Fig. 3. In particular, Fig. 5 depicts the integrated temperature profiles when $\Delta L/L = 0.1$ (solid line), 0.3 (dotted line), and 0.5 (dashed line). We may see that the form of the temperature variation is highly sensitive to the spatial distribution of the heating. As a consequence of distributing the pulses on a broader region, hotter loops are produced as confirmed by the $\Delta L/L = 0.3$ and 0.5 calculation models. We also notice that the upper, hot loop segments become progressively less flat when the impulsive heating is more broadly distributed along the loop. In particular, the form of the temperature variation for the $\Delta L/L = 0.5$ loop model is similar to that corresponding to a uniformly heated loop as described by Priest et al. (1998) from X-ray observations of the diffuse corona. Moreover, the results also imply that a quasi-isothermal temperature distribution along

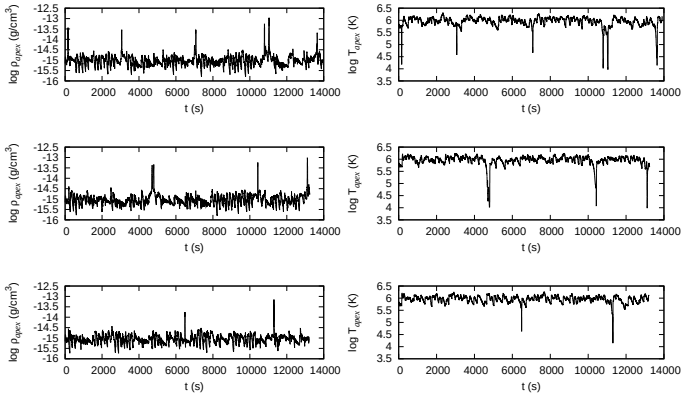

Figure 4: *Variation of the apex density (left panels) and apex temperature (right panels) with time for three loop models of total length* $L = 10$ *Mm each, undergoing impulsive heating through the release of a large number of pulses. The spatio-temporal random distribution of the pulses differ for each model. In all cases, the pulses were injected over segments of length* $0.1L$ *from the loop's footpoints. The upper two panels correspond to the model evolution shown in Fig. 3.*

the loop length is a clear signature of the heating being more strongly concentrated at the footpoints as deduced by Aschwanden et al. (2001) from observations of *TRACE* loops. Finally, we note that when the heating is less concentrated at the footpoints, the occurrence of the rapid temperature depressions strongly diminishes. This result is consistent with the observational lack of detected strong variability in the X-ray and EUV emission lines at higher coronal temperatures (Kjeldseth-Moe & Brekke 1998; Schrijver 2001).

4 Conclusions

In this paper we have described the evolution of a coronal loop model that has been heated impulsively near the footpoints.

It was found that successive microscale energy inputs are quite capable of heating up the loop plasma to typical coronal temperatures, which are, in general, maintained for the whole duration of the impulsive heating. As long as the elapsing time between successive pulses is increased in the 5 and 10 Mm models to ≈ 175 and ≈ 215 s, respectively, the loop heats up towards progressively lower temperatures. For elapsing

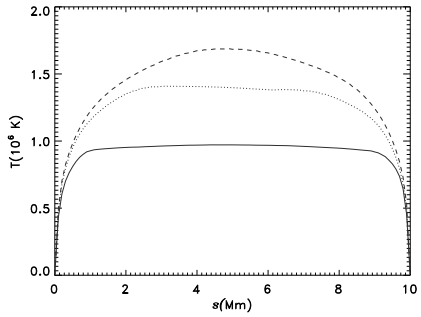

Figure 5: *Time integrated temperature profiles for the model evolution of Fig. 3, when the length of the bottom loop segments over which the pulses are randomly distributed is* 0.1 *(solid line),* 0.3 *(dotted line), and* $0.5L$ *(dashed line). The temperature is given in units of* 10^6 *K. In each case, the time integration was performed over the whole evolution (*$\approx$ 15000 *s).*

times longer than these critical values, coronal temperatures can no longer be maintained as radiative cooling proceeds faster than impulsive heating. As a consequence, the loop apex undergoes catastrophic cooling well below the initial state to typical chromospheric temperatures ($\sim 10^4$ K). The precise value of the critical elapsing time is seen to increase with increasing total loop length. In particular, catastrophic cooling in the 20 and 30 Mm loop models occurs at about 240 and 263 s, respectively.

Finally, loop simulations with a large number of pulses, having a fully random spatio-temporal distribution, confirm previous findings that the plasma would stay at coronal temperatures during the impulsive heating stage. Variations in the randomness of the heat releases produce qualitatively similar evolutions, differing mainly in the spatio-temporal distribution of the localized thermal bumps that appear randomly along the hottest loop segments. The model calculations also predict the occurrence of sporadic and very rapid temperature depressions near the loop apex, which are always accompanied by equally rapid rises of the apex density. These depressions may involve strong temperature variations, most of them from $\sim 1.5\times10^6$ to $\sim 10^4$ K, which may last from about 3 to 10 min, and their number may be sensitive to the details of the spatio-temporal distribution of the microscale heating. This behavior may be related to the observed rapid time variability of coronal loops inferred from *SOHO*-CDS observations in active regions of the solar atmosphere (Kjeldseth-Moe & Brekke 1998; Schrijver 2001). Moreover, when the pulses are less concentrated near the loop's footpoints, the evolution produces hotter loops and progressively less flat temperature profiles in the upper parts of the loop along with an appreciably reduced number of

the temperature depressions. This latter feature is consistent with the observational lack of strong variability at very high coronal temperatures (Kjeldseth-Moe & Brekke 1998; Schrijver 2001).

Acknowledgement

The author thanks to the British Council and the Particle Physics and Astronomy Research Council (PPARC), UK, for the financial support.

References

Aschwanden, M. J., Schrijver, C. J., & Alexander, D. 2001, ApJ, 550, 1036

Bradshaw, S. J., & Mason, H. E. 2003, A&A, 407, 1127

Erdélyi, R., De Pontieu, B., & Roussev, L. M. 2001, in ASP Conf. Ser. 223, Cool Stars, Stellar Systems, and the Sun: 11th Cambridge Workshop, ed. R. J. García López, R. S. Polidan, & R. W. Pogge (San Francisco: ASP), 619

Harrison, R. A., & Hood, A. W. 2002, A&A, 392, 319

Innes, D. E., Inhester, B., Axford, W. I., & Wilhelm, K. 1997, Nature, 386, 811

Kjeldseth-Moe, O., & Brekke, P. 1998, Sol. Phys., 182, 73

Mendoza-Briceño, C. A., Erdélyi, R., & Sigalotti, L. Di G. 2002, ApJ, 579, L49

Mendoza-Briceño, C. A., Sigalotti, L. Di G., & Erdélyi, R. 2003, Adv. Space Res., 32(6), 995

Parker, E. N. 1988, ApJ, 330, 474

Patsourakos, S., & Vial, J.-C. 2002, A&A, 385, 1073

Pérez, M. E., Doyle, J. G., Erdélyi, R., & Sarro, L. M. 1999, A&A, 342, 279

Priest, E. R., Foley, C. R., Heyvaerst, J., Arber, T. D., Culhane, J. L., & Acton, L. W. 1998, Nature, 393, 545

Roussev, I., Galsgaard, K., Erdélyi, R., & Doyle, J. G. 2001a, A&A, 370, 298

Roussev, I., Doyle, J. G., Galsgaard, K., & Erdélyi, R. 2001b, A&A, 380, 719

Sarro, L. M., Erdélyi, R., Doyle, J. G., & Pérez, M. E. 1999, A&A, 351, 721

Schrijver, C. J. 2001, Sol. Phys., 198, 325

Sigalotti, L. Di G., & Mendoza-Briceño, C. A. 2003, A&A, 397, 1083

Teriaca, L., Doyle, J. G., Erdélyi, R., & Sarro, L. M. 1999, A&A, 52, L99

Walsh, R. W., & Galsgaard, K. 2001, in Solar Encounter: Proc. First Solar Orbiter Workshop, ed. B. Battrick & H. Sawaya-Lacoste (ESA SP-493; Noordwijk: ESA), 427